Electron Impact Ionization of Sodium Rydberg Atoms below 2 eV

K. Nagesha and K. B. MacAdam

Department of Physics and Astronomy, University of Kentucky, Lexington, Kentucky 40506-0055, USA

(Received 16 May 2003; published 12 September 2003)

We have observed electron impact ionization of highly excited sodium Rydberg atoms in *ns* and *nd* states, $n = 35$–51, below $E = 2$ eV electron kinetic energy with energy resolution 0.25 eV. Measured absolute cross sections near 0 eV range from $\sigma_{35d} \approx 7 \times 10^{-10}$ to $\sigma_{50d} \approx 4 \times 10^{-9}$ cm^2. The energy dependence is consistent with that of widely used binary encounter approximation cross sections, and σ_n follows a power law in n. The measured cross sections are 14 to 24 times larger than theoretically predicted values. This enhancement may signal the effect of large polarizabilities of high Rydberg states not yet accounted for in ionization theories.

DOI: 10.1103/PhysRevLett.91.113202 PACS numbers: 34.80.Dp, 34.60.+z

Electron impact ionization (EII) is a vital process in gas discharges and plasmas [1–3]. Accurate EII cross sections (EIICSs) for ground and excited states of atoms and molecules are important in modeling arcs [4], discharges [5], plasmas [6], the solar atmosphere [7] and astrophysical media [8], as well as in spectroscopy [9] of ionized media and benchmarking theoretical predictions [10]. Most EII studies have involved ground states [1,2]. Only a handful of EII studies have been carried out on excited states, and those only spanning a small range of low principal quantum number n in different targets, viz., rare gases [3], some alkaline earths [11], and alkali metals [12,13]. These studies have revealed a shift of the peak in EIICS to lower electron energies with increasing n and enlarged maximum values, corresponding to decreasing ionization energies [3]. Ionization thresholds for low lying target states studied to date were several eV, and EIICSs had magnitudes of several $\times 10^{-16}$ cm^2. High Rydberg states (HRSs) of atoms and molecules, e.g., having $n \geq 30$, exist alongside low-energy electrons in most plasmas of laboratory, upper atmosphere, astrophysical, and technological interest [1–9]. HRSs have binding energies much less than 1 eV and act as excellent electron donors [3]. HRSs and ions are highly reactive in the presence of low-energy electrons, leading to ionization and recombination [14], and can significantly affect the properties of ionized media involving excited species [3]. Modeling of such media [4–9] relies on empirical formulas for low and high lying states [15–17], despite the absence of verification through experimental absolute EIICSs of HRSs at any impact energy. Field- and photon-induced Rydberg ionization mechanisms have been known [18] for a long time, but to our knowledge no observations of EII in state-selected HRSs at any energy have been published. Previous electron impact studies with atomic HRSs mostly involved n and ℓ changing in the target state at far higher energies (25–600 eV) [19,20]. Here we report experimental observation of the ionization of Na Rydberg atoms upon direct electron impact. We present absolute EIICSs and their energy and n dependence below 2 eV for Na *ns* and *nd* states, $n = 35$–51. Our results show an enhancement factor of 14 to 24 compared to values predicted by widely accepted theoretical models.

Experiments were carried out in a new crossed-beam collision chamber evacuated to 10^{-9} torr by a helium cryopump. A sodium vapor beam was collimated by an aperture placed 15 cm from the target center. The electron beam was generated and collimated to 1 mm diameter in a trochoidal electron monochromator (TEM) [21] employing a uniform magnetic field of 80 G. We optimized the TEM design to yield electron beam currents sufficient (up to 300 nA) to observe low-energy electron-Rydberg collision signals above noise levels, although this unavoidably set a limit on the attainable energy resolution (~ 250 meV). The benefit of the TEM was in being able to maintain nearly constant electron flux down to 0 eV. The electron beam current was monitored by a Faraday cup placed beyond the interaction center (Fig. 1). A shielding grid placed in front of the cup confirmed the electron beam size: The e^- beam confined against spreading by the magnetic guide field imprinted a mark of 1 mm diameter on the mesh, indicating that the beam did not significantly expand during 8 cm travel through the interaction region. Two parallel grids, G1 and G2 in Fig. 1, were placed symmetrically about the interaction center for ion extraction and state-selective field ionization (SFI) [22]. A high-current channel electron multiplier (CEM) detector operated in analog mode was shielded and positioned 5 mm behind grid G2. In the experiments, Na was excited stepwise to a selected Rydberg state using two pulsed (30 Hz) dye-laser beams (pumped together by a Q-switched Nd:YAG laser) counterpropagating along the Na beam, as shown by a horizontal ribbon in Fig. 1. The yellow laser tuned to wavelengths 589.6 or 589.0 nm excited Na atoms from the ground state to the $3^2P_{1/2}$ or $3^2P_{3/2}$ state, respectively. The tunable blue laser flashing simultaneously at about 410 nm excited the $3P$ state to a

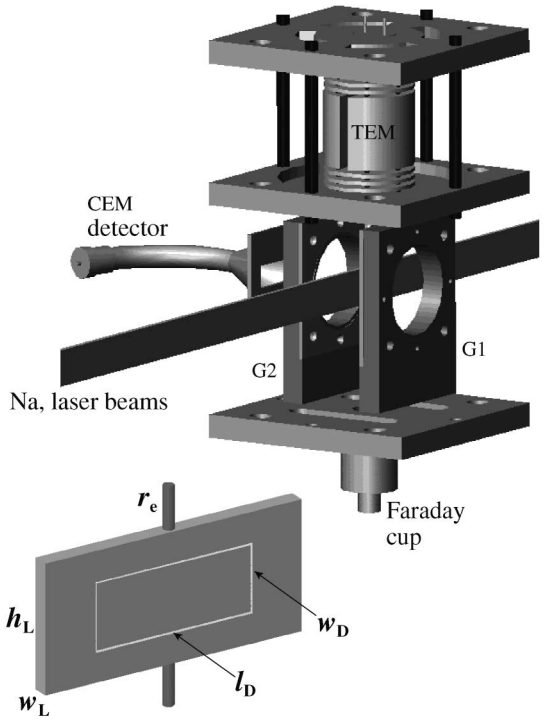

FIG. 1. Schematic of the interaction region. Counterpropagating laser and atomic beams are shown by a horizontal ribbon. G1 and G2 are extraction grids. Below: geometry for determining absolute cross sections: electron beam of radius r_e, Rydberg column with cross sectional area $w_L \times h_L$, and ion detection window $l_D \times w_D$.

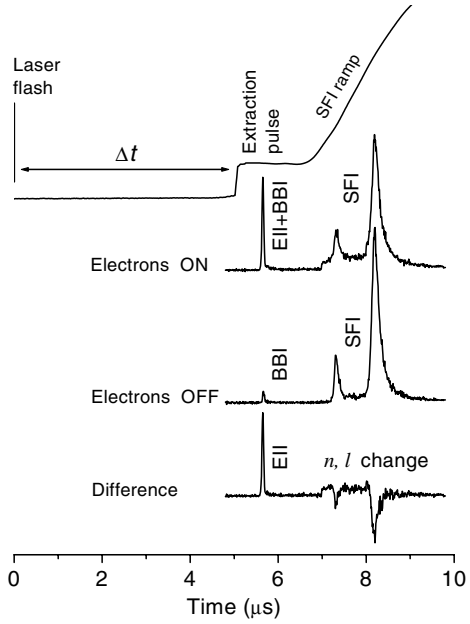

FIG. 2. The top curve, a graph of voltage on grid G1 (Fig. 1) vs time, illustrates the ion-extraction and the field-ionization scheme. Δt is the duration of electron-Rydberg interaction. The lower three curves are Na^+ ion CEM signals and their difference. The first peak in the "difference" signal is due to electron impact ionization.

desired ns or nd state, $n = 35$ to 51. The electron beam intersected the cloud of Rydberg atoms at a right angle from above.

In Fig. 2, the instant of laser flash marks the formation of Na Rydberg states. Electrons at kinetic energy E were allowed to pass through the Rydberg-atom region for several μs, as indicated by Δt in Fig. 2. Na^+ ions that accumulated during this interval were extracted into the CEM by applying a rectangular field pulse (30 V/cm, 1.5 μs) to grid G1 (Fig. 1), indicated in the top curve of Fig. 2. Ion extraction was followed immediately by a SFI voltage pulse applied to grid G1. The SFI pulse was an increasing ramp, which Stark-split the Rydberg levels and selectively ionized Stark multiplets [22], sweeping the resulting ions into the CEM detector. This measurement was repeated alternately with "electrons on" and "electrons off" for a large number of laser shots until a good signal-to-noise ratio was achieved in the ionization signals recorded by a digital storage oscilloscope.

Typical ionization signals are shown in Fig. 2. The area under the first peak, correlating with the extraction pulse, is proportional to the number of Na^+ ions produced during Δt, and the SFI signal area (S_{SFI}) is proportional to the number of residual Rydberg atoms. The first peak in the electrons on signal includes Na^+ ion signals due to both EII and room-temperature blackbody ionization (BBI) [22], while in the electrons off signal it corresponds to BBI only (S_{BBI}). The difference signal yields the EII contribution (S_{EII}) alone. The nonzero excursions of the difference signal in the SFI region indicate n and ℓ changes in target Rydberg atoms [19,20] that occur concurrently with EII. In this Letter we focus on EII.

We have devised a new method to extract absolute cross sections $\sigma(E)$ from ionization signals of Fig. 2, based on accurately controlled sizes of the interacting beams and the detection window as depicted in Fig. 1. The electron beam shown by a cylinder has a circular cross section of radius r_e. Lasers enter the chamber through a rectangular slit of area w_L (1.5 mm) $\times$ h_L (12 mm). Rydberg states are produced in the overlap region of laser and atomic beams through the middle of which the electron beam passes vertically downward. The CEM has a rectangular ion entrance aperture of area w_D (6.35 mm) $\times$ l_D (15.24 mm) serving as a detection window. Ions are produced by EII, BBI, and SFI, but only those in the volume defined by $w_L l_D w_D$ are detected by the CEM. Ions from both EII and BBI and residual neutral Rydberg atoms have merely thermal energies (velocities ≈ 1 mm/μs) until they are swept into the CEM by the ion sweep and SFI pulses, respectively.

Figure 1 indicates that Na^+ ions are produced due to EII in the electron-Rydberg overlap volume $\pi r_e^2 h_L$. However, only those produced in a smaller volume $\pi r_e^2 w_D$ are within the detection window and contribute to $S_{EII}(E)$. Signals $S_{SFI}(E)$ and S_{BBI} originate from

detection volume $w_L l_D w_D$. If $\rho_{Na^+}(E)$ and ρ_{Na^*} are ion and Rydberg-atom densities, respectively, then the rate of increase of the ionization fraction is a product of EIICS and the electron flux at energy E,

$$\frac{d}{dt}[\rho_{Na^+}(E)/\rho_{Na^*}] = \sigma(E) I_0(E)(q\pi r_e^2)^{-1}, \qquad (1)$$

where $I_0(E)$ is the electron beam current and q is the electronic charge. In our experiments the rate of increase is observed to be constant for $\Delta t \leq 6.5$ μs, from which we infer that ions produced early in the exposure time Δt have not yet drifted or recoiled out of view of the detector. Since $\rho_{Na^+}(E) \propto S_{EII}(E)(\pi r_e^2 w_D)^{-1}$ and $\rho_{Na^*} \propto [S_{SFI}(E) + S_{EII}(E) + S_{BBI}](w_L l_D w_D)^{-1}$, Eq. (1) is equivalent to

$$\sigma_{exp}(V_r) = \left(\frac{\mathsf{S}(V_r)}{\Delta t}\right)\left(\frac{q l_D w_L}{I_0(V_r)}\right). \qquad (2)$$

The experimental ionization fraction $\mathsf{S}(V_r) = S_{EII}(V_r)/[S_{SFI}(V_r) + S_{EII}(V_r) + S_{BBI}]$ is measured as a function of a stepped reference potential V_r applied to the TEM electron gun, which additively shifts the energy of electrons in the output beam. From it an experimental EIICS, $\sigma_{exp}(V_r)$, is obtained via Eq. (2). The procedure has eliminated the need to know the absolute Rydberg density as well as efficiencies for ion extraction and detection, extraction grid attenuation, and electronic amplification factors. The relationship between V_r and the true electron kinetic energy E is determined later in data analysis, in which a measured electron energy distribution is used and a voltage or energy offset is determined by fitting. Determination of accurate ion and Rydberg densities and electron-target beam overlap volume has previously been a difficult part of measuring absolute EIICSs for excited states [3]. It was experimentally confirmed, as expected, that $\mathsf{S}(V_r)$ is not affected by fluctuations in laser intensity and sodium beam density. Importantly, Eq. (2) is independent of the electron beam radius or cross sectional profile (when $2r_e < w_L$). We estimate that statistical errors amount to $\pm 20\%$ and systematic errors in determining the absolute experimental EIICS to another $\pm 20\%$.

The electron energy dependence of the EII signal was obtained by fixing $\Delta t = 6.0$ μs and scanning V_r, averaging over repeated runs. In Fig. 3 we show $\sigma_{exp}(V_r)$ for $45d$ excited via $3^2P_{1/2}$. The experimental cross section is strongly influenced by the e^- energy distribution and its offset; $\sigma_{exp}(V_r)$ exhibits a strong peak near $V_r = -0.45$ V. This corresponds well with the most probable energy $E \approx 0.5$ eV for the electrons emerging from the thermionic emitter and with the expectation that EII has a strong maximum just above threshold. $\sigma_{exp}(V_r)$ measured for the $45d$ state excited via $3^2P_{3/2}$ matched that shown in Fig. 3 for $3^2P_{1/2}$, as was expected. We have measured $\sigma_{exp}(V_r)$ for $35d$, $36s$, $38d$, $40d$, $41s$, $42d$, $45d$, $46s$, $48d$, $50d$, and $51s$ target states excited via $3^2P_{1/2}$. All curves

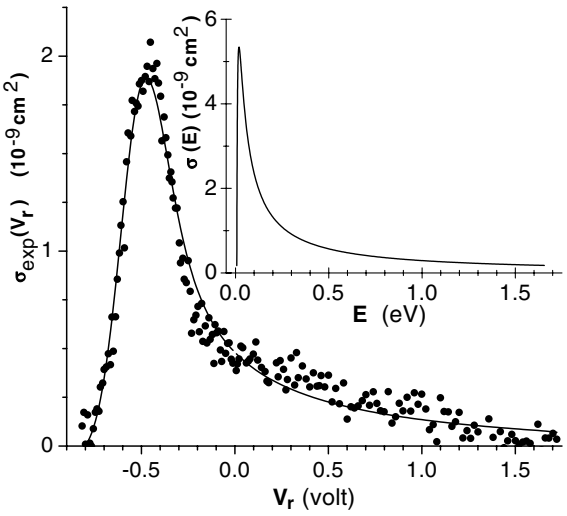

FIG. 3. Electron impact ionization cross section for the $45d$ state excited via $3^2P_{1/2}$: (dots and line) experimental data and fit to σ_{exp} using binary-encounter cross section VS [16], convoluted over electron energy. Inset: underlying VS cross section multiplied to fit the experimental results.

were similar in shape but had increased peak heights as n increased. The EII signal for $n < 35$ was too weak to measure while for $n > 51$ the blue laser linewidth did not adequately resolve nd and $(n+1)s$ states.

Vriens and Smeets [16] have provided a simple analytical formula that describes the EIICS from hydrogenic excited states based on the symmetrical model of the binary encounter approximation, adjusted for best agreement at the lowest energies with classical trajectory Monte Carlo calculations and experiments. The results are widely used for plasma modeling [4–9]. Their formula Eq. (2) in Ref. [16] (equation referred to here as VS) is applicable from threshold $E_n = (13.6 \text{ eV})/n^2$ up to tens of eV. For $n = 35$–51 the VS ionization cross sections reach maximum at energies a few times threshold and drop to half maximum before $E = 0.2$ eV.

Given the energy resolution in the present experiments we cannot make a critical test of the functional form of VS. Instead we assume that VS adequately represents the true EIICS except for an overall dimensionless multiplicative factor K, and we convolute VS with the energy distribution, which was determined independently in each set of runs by a Faraday-cup scan of transmitted electron current while V_r was stepped from negative to positive values through $E = 0$. The distributions were well described by Gaussians, whose widths we applied to the associated runs. We fit the Gaussian-convoluted VS model to the experimental $\sigma_{exp}(V_r)$ to find an optimal value of K and an energy offset E_0 that relates V_r to the true mean electron kinetic energy E according to $E = qV_r + E_0$.

Figure 3 shows the VS fit to the experimental cross section for $45d$. The underlying VS cross section, with

TABLE I. Electron impact ionization cross sections of Na($n\ell$) Rydberg states.

$n\ell$	σ_{exp} max. (10^{-9} cm^2)	σ(0.2 eV) (10^{-9} cm^2)	$\sigma(\tilde{v}=4)$ (10^{-9} cm^2)	K
35d	0.71	0.57	0.63	14.4
36s	0.76	0.53	0.57	13.5
38d	1.03	0.78	0.98	16.0
40d	1.14	0.75	1.04	13.8
41s	1.09	0.65	0.87	12.1
42d	1.42	1.09	1.63	17.9
45d	1.89	1.38	2.32	19.3
46s	1.92	1.23	2.04	17.5
48d	2.57	1.74	3.29	21.2
50d	3.52	2.17	4.41	24.2
51s	3.19	1.89	3.79	21.3

multiplier K and without energy broadening, is plotted also as a function of the derived true energy E. Based on our data K varies from about 14 (35d) to 24 (50d). We infer the empirical underlying cross section $\sigma(E)$ without electron energy broadening to be K times the corresponding VS cross section (see Table I).

From the VS fits we have determined the n dependences of σ_n, at a fixed energy 0.2 eV and at a fixed reduced velocity $\tilde{v} = 4.0$. [$\tilde{v}$ is the ratio of projectile speed to the root mean square orbital speed of the Rydberg electron. For hydrogen, $\tilde{v} = n\sqrt{E/(13.6\ \text{eV})}$.] Both are power laws of the form $\sigma_n \propto n^{\beta}$. At 0.2 eV, $\beta = 3.74 \pm 0.28$: This is at variance with VS, which gives an exponent 2.28 at this energy. σ_n at fixed reduced velocity rises with $\beta = 5.46 \pm 0.28$, instead of the VS or classical-scaling exponent exactly 4 at any fixed $\tilde{v}$.

The large discrepancy between measurements and VS could originate from the enormous polarizabilities of HRSs. Rydberg-state polarizabilities grow as n^7 [23] and contribute an attractive potential in charged particle impact that varies with distance as $1/r^4$. No systematic account has been made of polarizability in EII theory; Born-approximation variants, binary encounter, and classical trajectory calculations applicable to excited n, ℓ states contain no allowance for it. The corroboration of these theories for EII of ground or low-excited states, whose thresholds are much higher and polarizabilities are negligible, sheds no light on their accuracy for highly excited states, which is thus an open issue albeit one of considerable importance for laboratory, technological, and astrophysical plasma modeling.

Na Rydberg-atom EIICSs are by far the largest measured with any atom or state. We have observed energy-broadened EII cross sections that range from 7×10^{-10} cm^2 for 35d to 4×10^{-9} cm^2 for 50d at a small fraction of an eV above threshold, we have determined absolute values by direct calibration without normalization to other experimental or theoretical values, we have measured power-law n dependences, and we have found that the underlying EII cross sections of Na Rydberg states exceed those previously assumed in models based on low-n data by more than an order of magnitude.

The authors thank M. J. Cavagnero, R. G. Rolfes, and G. J. Ferland for helpful discussions. This work was supported in part by NSF Grant No. PHY-9987954.

[1] R. Hippler *et al.*, *Low Temperature Plasma Physics* (Wiley-VCH Verlag, Berlin, 2001).
[2] D. Salzmann, *Atomic Physics in Hot Plasmas* (Oxford University Press, New York, 1998).
[3] L. G. Christophorou and J. K. Olthoff, Adv. At. Mol. Opt. Phys. **44**, 155 (2001).
[4] K. T. A. L. Burm *et al.*, Plasma Sources Sci. Technol. **7**, 395 (1998).
[5] G. G. Lister, J. J. Curry, and J. E. Lawler, Phys. Rev. E **62**, 5576 (2000).
[6] C. Lao *et al.*, J. Appl. Phys. **87**, 7652 (2000).
[7] A. A. Mihajlov *et al.*, Astron. Astrophys. **324**, 1206 (1997).
[8] J.W. Ferguson and G. J. Ferland, Astrophys. J. **479**, 363 (1997).
[9] T. Fujimoto and R.W. P. McWhirter, Phys. Rev. A **42**, 6588 (1990).
[10] J. Colgan *et al.*, Phys. Rev. Lett. **87**, 213201 (2001).
[11] S. Trajmar, J. C. Nickel, and T. Antoni, Phys. Rev. A **34**, 5154 (1986).
[12] A. R. Johnston and P. D. Burrow, Phys. Rev. A **51**, R1735 (1995); W. S. Tan *et al.*, Phys. Rev. A **54**, R3710 (1996).
[13] M. L. Keeler, L.W. Anderson, and C. C. Lin, Phys. Rev. Lett. **85**, 3353 (2000); R. S. Schappe *et al.*, Phys. Rev. Lett. **76**, 4328 (1996).
[14] M. R. Flannery, Adv. At. Mol. Opt. Phys. **32**, 117 (1994).
[15] L. C. Johnson, Astrophys. J. **174**, 227 (1972).
[16] L. Vriens and A. H. M. Smeets, Phys. Rev. A **22**, 940 (1980).
[17] I. L. Beigman, V. P. Shevelko, and H. Tawara, Phys. Scr. **53**, 534 (1996).
[18] G. M. Lankhuijzen and L. D. Noordam, Adv. At. Mol. Opt. Phys. **38**, 121 (1997).
[19] G.W. Foltz *et al.*, Phys. Rev. A **25**, 187 (1982).
[20] R. G. Rolfes *et al.*, J. Phys. B **26**, 2191 (1993).
[21] A. Stamatovic and G. J. Schulz, Rev. Sci. Instrum. **41**, 423 (1970).
[22] T. F. Gallagher, *Rydberg Atoms* (Cambridge University Press, New York, 1994).
[23] C. Fabre and S. Haroche, in *Rydberg States of Atoms and Molecules*, edited by R. F. Stebbings and F. B. Dunning (Cambridge University Press, New York, 1983), p. 117.